

Smoothed Particle Hydrodynamics Simulations of Apsidal and Nodal Superhumps

Matt A. Wood, Michele M. Montgomery

*Department of Physics and Space Sciences and SARA Observatory,
Florida Institute of Technology,
Melbourne, FL 32901-6975, USA,
wood@astro.fit.edu, michele@astro.fit.edu*

and

James C. Simpson

*Computer Sciences Raytheon, P.O. Box 4127, CSR 1310, Patrick Air Force Base, FL 32925-0127,
james.simpson@patrick.af.mil*

ABSTRACT

In recent years a handful of systems have been observed to show “negative” (nodal) superhumps, with periods slightly *shorter* than the orbital period. It has been suggested that these modes are a consequence of the slow retrograde precession of the line of nodes in a disk tilted with respect to the orbital plane. Our simulations confirm and refine this model: they suggest a roughly axisymmetric, retrogradely-precessing, tilted disk that is driven at a period slightly less than *half* the orbital period as the tidal field of the orbiting secondary encounters in turn the two halves of the disk above and below the midplane. Each of these passings leads to viscous dissipation on one face of an optically-thick disk — observers on opposite sides of the disk would each observe one brightening per orbit, but 180° out of phase with each other.

Subject headings: accretion disks – binaries: close – cataclysmic variables – methods: numerical – hydrodynamics

To appear in *The Astrophysical Journal Letters*

1. Introduction

Cataclysmic variable (CV) systems in the mass-ratio range $q \equiv M_2/M_1 \lesssim 0.33$ (e.g., Murray 2000) are observed to show the disk oscillations known as superhumps (see Warner 1995 and Patterson 1999 for recent reviews). First observed in the SU Ursae Majoris stars, *common* (a.k.a. *positive* or *apsidal*) superhumps have periods a few percent in excess of their system orbital periods. The story and classification scheme, however, have in recent years become more complicated. First, some old novae and nova-likes show “permanent” positive superhumps indicating a high and roughly constant mass transfer rate, e.g., V603 Aquilae (Patterson et al. 1993, 1997) V795 Herculis (Patterson & Skillman 1994), H 0551-819 (Patterson 1995), MV Lyrae (Skillman, Patterson, & Thorstensen 1995), and V1974 Cygni (Retter, Leibowitz, & Ofek 1997; Skillman et al. 1997). Second, a few systems, including V603 Aql, H 0551-819, V503 Cyg (Harvey et al. 1995), V1159 Orionis (Patterson et al. 1995), TT Arietis (Skillman et al. 1998; Kraicheva et al. 1999), AM CVn (Skillman et al. 1999) display so-called *negative* (or nodal) superhumps, which have periods a few percent *shorter* than the orbital period.

The favored model explaining positive superhumps is that for systems in the range $0.03 \lesssim q \lesssim 0.33$ with high mass transfer rates and viscosities, the outer disk can expand to the radius near the 3:1 eccentric inner Lindblad resonance (just outside the 3:1 corotation radius) where it can be driven periodically by the tidal field of the orbiting secondary (Whitehurst 1988, 1994; Hirose & Osaki 1990; Lubow 1991a,b; Murray 1996). Numerical simulations by Simpson & Wood (1998) show that over one oscillation period, as viewed face-on, the disk is pulled into a distorted, elongated shape followed by relaxation back to a nearly circular shape, and that during this oscillation, the spiral shock pattern advances 180° in the slowly precessing frame (n.b., spectroscopic time-series of an eclipsing superhumper may reveal this motion). Simulations further suggest that viscous energy dissipation through the cycle is the dominant source of the observed photometric oscillations and is highest when the disk is maximally distorted and the streamlines are most non-circular.

Because both modes have been observed *simultaneously* in several of the systems listed above (e.g., V603 Aql, V1159 Ori, H 0551-819, and V503 Cyg),

the physical origin of the negative superhumps must be distinct from the above mechanism. The model suggested by Harvey et al. (1995) invokes the retrograde precession of the *line of nodes* in an accretion disk *tilted* with respect to the orbital plane (see also Bonnet-Bidaud, Motch, & Mouchet 1985 and Barrett, O’Donoghue, & Warner 1988). Having identified physical processes associated with each superhump mode, we hereafter follow Harvey et al. (1995) and refer to positive and negative superhump modes as apsidal and nodal, respectively, thereby avoiding the awkward term “negative period excess.”

The linear theory of tilted disks (Papaloizou & Pringle 1983; Papaloizou & Terquem 1995) suggests that for the disk to precess as a solid body, the sound crossing timescale must be shorter than the precession timescale, a condition that is well satisfied in our simulations. Larwood et al. (1996) studied the general dynamics of tilted disks using the method of smoothed particle hydrodynamics (SPH), and found that for a constant surface density Σ disk tilted at angle δ with respect to the orbital plane, the nodal precessional rate is given by

$$\frac{\omega_p}{\Omega(R)} = -\frac{15}{32}q\beta^3 \cos \delta \quad (1)$$

where $\beta \equiv R_d/a$ is the disk radius in units of the orbital separation, and where a ratio of specific heats $\gamma = 5/3$ was assumed. For typical values, $q = 0.25$, $\beta = 0.4$, $\Omega(R) = 3\Omega_{\text{orb}}$, equation 1 gives ~ 40 orbits per precession period, which is in factor-of-two agreement with observations and our simulations below.

In this work we report the preliminary results of a large parametric study (Montgomery, Wood, & Simpson 2000, in preparation) exploring the dynamics of tilted disks and the origin of the nodal superhump phenomenon. Our primary result is that the model of a tidally-driven retrogradely-precessing disk is basically confirmed, but that the driving frequency is slightly higher than twice per orbit as each of the two out-of-orbital-plane halves of the disk are perturbed sequentially and out of phase with each other. Because we receive photons from only one face of an optically-thick disk in superoutburst, we *measure* a photometric period which is just shorter than the orbital period. This model predicts that the waveform observed from a tilted disk that is optically-thin or viewed from high inclination should be approximately doubly-periodic each orbit.

2. General Characteristics of the SPH Models

Smoothed particle hydrodynamics (SPH) provides an effective tool for modeling accretion disks in general, and those arising in binary star systems in particular (for a review, see Monaghan 1992). We use the code described in Simpson (1995) and Simpson & Wood (1998). The code is based on particle-particle interactions within the disk and the mass transfer stream, with the only remaining body forces being the gravitational attraction of the two stars (i.e., disk self-gravity is negligible and ignored). In the models reported here, particles are injected into the disk through the binary’s inner Lagrangian (L_1) point at a rate of 2,000 particles per orbit until the maximum of 25,000 particles is reached. The number of particles is kept constant after this point by inserting a new particle whenever an already existing particle leaves the system by accretion or ejection from the computational space. We note that once equilibrium is established, the typical particle injection rate through L_1 is a nearly-constant 280 particles per orbit (1.4 per system timestep), giving a mean particle lifetime of 89.4 orbits from injection to accretion. At this point the disk is at the same equilibrium as if we had *set* the injection rate to a constant 280 particles per orbit.

The fundamental timestep for the simulations is $P_{\text{orb}}/200$, and individual particles can have shorter timesteps if needed, in steps of factors of 2. All particles in the simulation have identical smoothing lengths h for computational efficiency. We note that although our constant- h disks are somewhat under-resolved in the inner disk region, the superhump oscillations are located in the outer disk and are well-resolved.

For the runs presented here we assume an ideal gamma-law equation of state $P = (\gamma - 1)\rho u$, where u is the internal energy and where we use $\gamma = 1.01$. The artificial viscosity prescription used is that of Lattanzio et al. (1986) with $\alpha = 0.5$, $\beta = 0.5$, and $\eta = 0.1h$, as recommended by Lombardi et al. (1999).

As in Simpson & Wood (1998), we calculate an energy production time series — effectively a bolometric light curve — by assuming that the instantaneous disk luminosity is proportional to the change in the summed internal energy change of all particles integrated over the previous system timestep. The internal energy change is typically dominated by viscous energy dissipation, but $P dV$ work also contributes.

We use Fourier analysis to determine the frequencies at which the disk is driven by the tidal field of the secondary.

3. Results

3.1. The Reference Simulation Run

In this work we report the results for a $q = 0.25$ system with assumed masses $M_1 = 0.8M_\odot$ and $M_2 = 0.2M_\odot$. With our choice of secondary mass-radius relationship $R_2 = (M_2/M_\odot)^{13/15}R_\odot$ (Warner 1995, §2.8.3) and the relation for the volume radius of the secondary’s Roche lobe (Eggleton 1983)

$$\frac{R_2}{a} = \frac{0.49q^{2/3}}{0.6q^{2/3} + \ln(1 + q^{1/3})}, \quad (2)$$

our simulation unit length scales to $a = 0.93R_\odot$ and period 2π scales to $P_{\text{orb}} = 2.47$ hr. We note that our results below for the disk oscillation and precession frequencies in units of orb^{-1} would be unchanged for a simulation with $M_1 = 0.6M_\odot$, $M_2 = 0.15M_\odot$, and $P_{\text{orb}} = 2.0$ hr — the reader should place no special significance on the period here falling in the CV period gap.

Figure 1 shows the simulation light curve of the $q = 0.25$ apsidal superhump oscillation out to orbit 250, at which point the waveform is essentially stationary. For the purposes display only, we sum 10 points to suppress the high-frequency noise but the “data” are otherwise unprocessed. Each point is thus a relative integral average over an interval $P_{\text{orb}}/20$.

The apsidal superhumps reach observable amplitude near orbit 110. As the oscillation grows the global dissipation rate and mass flux through the disk rises, increasing the overall disk energy production (luminosity). The system is eventually forced into a state of dynamical equilibrium near orbit 200. The artificial light curves of the apsidal superhumps are double humped and reminiscent of published lightcurves.

The Fourier amplitude spectrum of orbits 200 to 300 is shown in the top panel of Figure 2. The double-humped profile yields a second harmonic of amplitude comparable to that of the fundamental frequency ν_a . The third through fifth harmonics are also clearly present with decreasing amplitudes. The frequencies of the peaks in this Figure are listed in Table 1.

3.2. Dynamics of a Tilted Disk

To test the idea that the origin of negative (nodal) superhumps is the periodic tidal stressing of a tilted disk with a regressing line of nodes, we first artificially rotate the position and velocity vectors of all particles by 5° at the end of orbit 200, where the rotation is about the line perpendicular to the line of stellar centers and passing through the primary. Running the simulation again to orbit 300, we obtained the Fourier transform in the middle panel of Figure 2. We thought at first the power at just above the orbital frequency was the nodal superhump frequency, but did not understand the physical origin of the other new peaks. We then tilted the disk at orbit 40 (well before the onset of the apsidal mode) allowed 10 orbits for transient effects to die away,

We show the energy-production curve from the second run for orbits 50 to 60 in Figure 3, where for display purposes, we have boxcar-smoothed the data with a filter of width 11 points (~ 0.05 orb). The troughs are easy to identify in the noisy data, and there is an oscillation evident with a period of roughly $\sim P_{\text{orb}}/2$. We calculated the Fourier transform of this energy-production curve from orbits 50 to 70 (bottom panel of Figure 2), stopping before the apsidal mode appears. *Only* the frequency with $P \sim P_{\text{orb}}/2$ and its second harmonic are detected.

At this point the underlying physics is clear: for an axisymmetric disk tilted about the primary, once per orbit the tidal field disturbs in turn the fluid flow in *each of the two* disk halves which are out of the orbital midplane and separated by the line of nodes. Each tidal disturbance is asymmetrical with respect to the disk midplane in that it affects the side facing the orbital midplane more than the opposite side of the disk. For an optically-thick disk in superoutburst, only photons from one side of the disk are observed, and so the observed nodal superhump periods are just shorter than once per orbit as the tilted disk precesses in a direction opposite the the fluid flow in the disk. To maintain consistency with the observational literature, we have labeled the main peak in the bottom transform $2\nu_n$. The location of what would be the observed nodal superhump frequency is marked with a dotted line, and is included in brackets in Table 1.

Figure 4 shows 5 sideview snapshots over a full nodal-precession period of $P_{np} \approx 24$ orbits for the $q = 0.25$ disk. The wobble is obvious. Because mass is added at the disk midplane, the tilt must decay

with time. To quantify the decay time scale, we ran this simulation out to orbit 400, and computed the Fourier amplitude spectra of orbits 250-300, 300-350 and 350-400. Assuming an exponential decay of the form $A(t_2) = A(t_1)e^{-\Delta t/\tau_d}$ with times at the centers of the above intervals, we use the amplitudes of the $2\nu_n$ peak in the three spectra ($A = 0.0104, 0.00714,$ and 0.00492 , respectively) to derive a decay time scale $\tau_d = 134$ orb. The corresponding ‘‘half-life’’ of the tilt decay, $\tau_{1/2} = \ln 2 \cdot \tau_d = 93$ orb, is very nearly the mean particle lifetime, as it must be from conservation of angular momentum arguments.

Now we can fully understand the Fourier transform of the reference disk tilted at orbit 200 and spanning orbits 200 to 300 (Figure 2, middle panel). First, tilting the disk did not significantly affect the frequencies of the apsidal superhump modes. Second, the power at the frequencies $2\nu_n - \nu_a$ and $2\nu_n + \nu_a$ (see Table 1) are linear combination frequencies resulting from the non-linear response of viscous dissipation in a disk which is precessing in opposite directions simultaneously and suffering tidal driving from the orbit of the secondary. We note that while the $2\nu_n + \nu_a$ peak is small in this transform, it is quite pronounced in disks with larger tilts.

3.3. On Generating a Tilted Disk

Lubow (1992) explored the growth rate of the tilt instability mode and found it to be $\sim 1/50$ -th that of the apsidal superhump mode growth rate. Murray & Armitage (1999) confirmed a consistent-with-zero growth rate mode using three-dimensional smoothed particle hydrodynamics (SPH) simulations where particles were injected into the disk at the circularization radius after an initial burst of particles to build the disk rapidly.

Several models have been suggested to generate tilted disks in cataclysmic variables, including an L_1 point effectively displaced out of the orbital plane as a result of channeling of the accretion flow near L_1 by magnetic activity associated with the mass-losing secondary (see, e.g., Barrett et al. 1988). As a simple test of this idea, we ran a simulation with the same parameters as our reference run above and another with $q = 0.05$, but with the L_1 injection point displaced in z by $0.05a$. The accretion stream passes through the disk midplane and impacts the disk on the side opposite the displaced L_1 point, and at a radius of about one-third the disk radius. Because the stream does not impact the disk rim, the disk radius

grows faster than in the reference simulation run, and common superhumps onset at about orbit 50 versus orbit 110 for the reference run. However, *we find no significant power at the frequency $2\nu_n$* in the amplitude spectrum of either simulation run as a result of displacing the L_1 point in a simulation run for 100 orbits.

If local magnetic field evolution and recombination contributes to the fluid viscosity and disk energetics, it is quite plausible that an outburst event could be asymmetrical with respect to the disk midplane and hence result in a tilted disk. Our code is not sufficient to explore this idea, however, so for now the origin of the disk tilt remains a puzzle.

4. Summary

Although these are preliminary results, it appears the tilted-disk model neatly explains many of the observational characteristics of nodal (“negative”) superhumps, and also suggests further observational and numerical tests. Our findings here can be summarized as follows.

- The results are consistent with the nodal regression model for the origin of negative superhumps. We tilted a disk both before and after the development of common apsidal superhump oscillations, and find power at twice the expected (observed) nodal superhump frequency. In superoutburst the disk is optically thick and so we observe only one face and hence only a single nodal mode brightening event per orbit — the other occurs on the opposite (hidden) face of the disk and is 180° out of phase. This model predicts that optically thin and/or edge-on tilted disks should display power at $2\nu_n$.
- In disks oscillating in both nodal and apsidal modes simultaneously, there is also power at the combination frequencies $2\nu_n - \nu_a$ and $2\nu_n + \nu_a$. These combination modes have not yet been identified in nature, but if demonstrated would provide additional support for this model.
- In our simulations, where we keep the particle number constant, the amplitude of the nodal mode decreases on a timescale of ~ 1000 orbits (several weeks if scaled to a physical orbital period). This is consistent with the observations, where the nodal superhump modes appear to

have a much longer decay time than the apsidal modes.

- The origin of the disk tilt remains an open question. Simply displacing the L_1 point out of the orbital midplane does not appear to be sufficient to generate a tilted disk, but more simulations are required.

We thank Fred Ringwald, Joe Patterson, Darragh O’Donoghue, and Shannon Baker-Branstetter for useful discussions. We also thank the anonymous referee. This work was supported in part by NASA through grant NAG 5-3103.

REFERENCES

- Barrett, P., O'Donoghue, D., & Warner, B. 1988, MNRAS, 233, 759
- Bonnet-Bidaud, J. M., Motch, C., & Mouchet, M., 1985, A&A, 143, 313
- Eggleton, P. P. 1983, ApJ, 268, 368
- Harvey, D., Skillman, D. R., Patterson, J., & Ringwald, F. A. 1995, PASP 107, 551
- Hirose, M., & Osaki, Y. 1990, PASJ, 42, 135
- Kraicheva, Z., Stanishev, V., Genkov, V., Iliev, L. 1999, A&A, 351, 607
- Larwood, J. D., Nelson, R. P., Papaloizou, J. C. B., Terquem, C. 1996, MNRAS, 282, 597
- Lattanzio, J. C., Monaghan, J. J., Pongracic, H., & Schwarz, M. P. 1986, J. Sci. Stat. Comput., 7, 591
- Lombardi, J. C., Jr., Sills, A., Frederic A. Rasio, F. A., & Shapiro, S. L. 1999, J. Comp. Phys., 152, 687
- Lubow, S. H. 1991a, ApJ, 381, 259
- Lubow, S. H. 1991b, ApJ, 381, 268
- Lubow, S. H. 1992, ApJ, 398, 525
- Monaghan, J. J. 1992, ARA&A, 30, 543
- Murray, J. R. 1996, MNRAS, 279, 402
- Murray, J. R. 2000, MNRAS, in press
- Murray, J. R. & Armitage, P. J. 1999, MNRAS, 300, 561
- Papaloizou, J. C. B., & Pringle, J. E. 1983, MNRAS, 202, 1181
- Papaloizou, J. C. B., & Terquem, C. 1995, MNRAS, 274, 987
- Patterson, J. 1995, PASP, 107, 657
- Patterson, J. 1999, PASP, 110, 1132
- Patterson, J., Jablonski, F., Koen, C., O'Donoghue, D., & Skillman, D. R. 1995, PASP, 107, 1183
- Patterson, J., Kemp, J., Saad, J., Skillman, D. R., Harvey, D., Fried, R., Thorstensen, J. R., & Ashley, R. 1997, PASP, 109, 468.
- Patterson, J., & Skillman, D. R. 1994, PASP, 106, 1141
- Patterson, J., Thomas, G., Skillman, D. R., & Diaz, M. 1993, ApJS, 86, 235
- Retter, A., Leibowitz, E. M., & Ofek, E. O. 1997, MNRAS, 286, 745
- Simpson, J. C. 1995, ApJ, 448, 822
- Simpson, J. C., & Wood, M. A. 1998, ApJ, 506, 360
- Skillman, D. R., Harvey, D., Patterson, J., & Vanmunster, T. 1997, 109, 114
- Skillman, D. R., Patterson, J., Kemp, J., Harvey, D. A., Fried, R. E., Retter, A., Lipkin, Y., & Vanmunster, T. 1999, ApJ, 111, 1281
- Skillman, D. R., Patterson, J., & Thorstensen, J. R. 1995, PASP, 107, 545
- Skillman, D. R., et al. 1998, ApJL, 503, 67
- Warner, B. 1995, Cataclysmic Variable Stars (New York: Cambridge U. Press)
- Whitehurst, R. 1988, MNRAS, 232, 35
- Whitehurst, R. 1994, MNRAS, 266, 35

TABLE 1
 APSIDAL AND NODAL MODE FREQUENCIES

Mode	Frequency ^a (orb ⁻¹)	Fractional Amplitude
ν_a	0.92	0.030
$2\nu_a$	1.85	0.028
$3\nu_a$	2.77	0.010
$4\nu_a$	3.69	0.0052
$5\nu_a$	4.64	0.0025
$[\nu_n]$	[1.04]	...
$2\nu_n$	2.08	0.011
$4\nu_n$	4.14	0.0084
$2\nu_n - \nu_a$	1.15	0.0092
$2\nu_n + \nu_a$	3.01	0.0002

^aThe uncertainties on all frequencies except $4\nu_n$ are 0.01 orb⁻¹ (100-orbit transform); uncertainty on $4\nu_n$ is 0.05 orb⁻¹ (20-orbit transform).

^bNot actually present in the Fourier transform of our simulation data, this is the nodal superhump frequency that would be observed (see text).

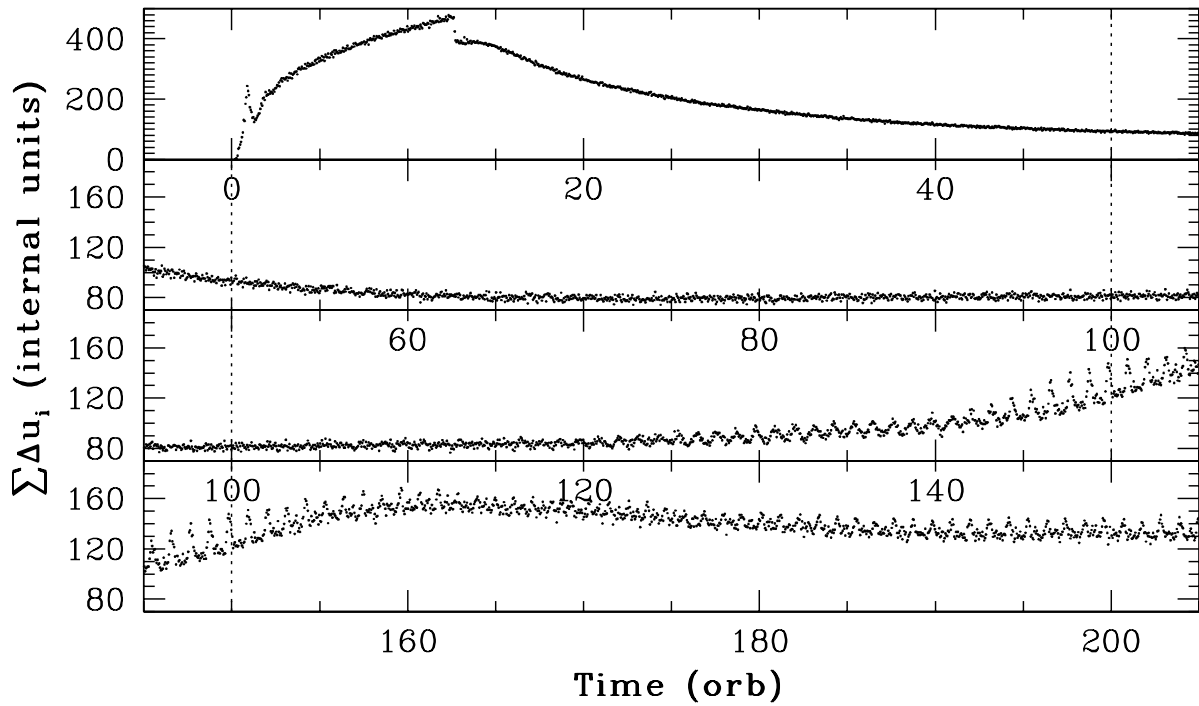


Fig. 1.— We show 200 orbits of the simulation light curve for a $q = 0.25$ system. Common (positive) superhumps are evident starting near orbit 110 and reach a dynamical equilibrium state near orbit 200. Note the vertical scale spans 500 units in the top panel and 100 units in the bottom 3 panels. Five orbits are repeated between panels for clarity.

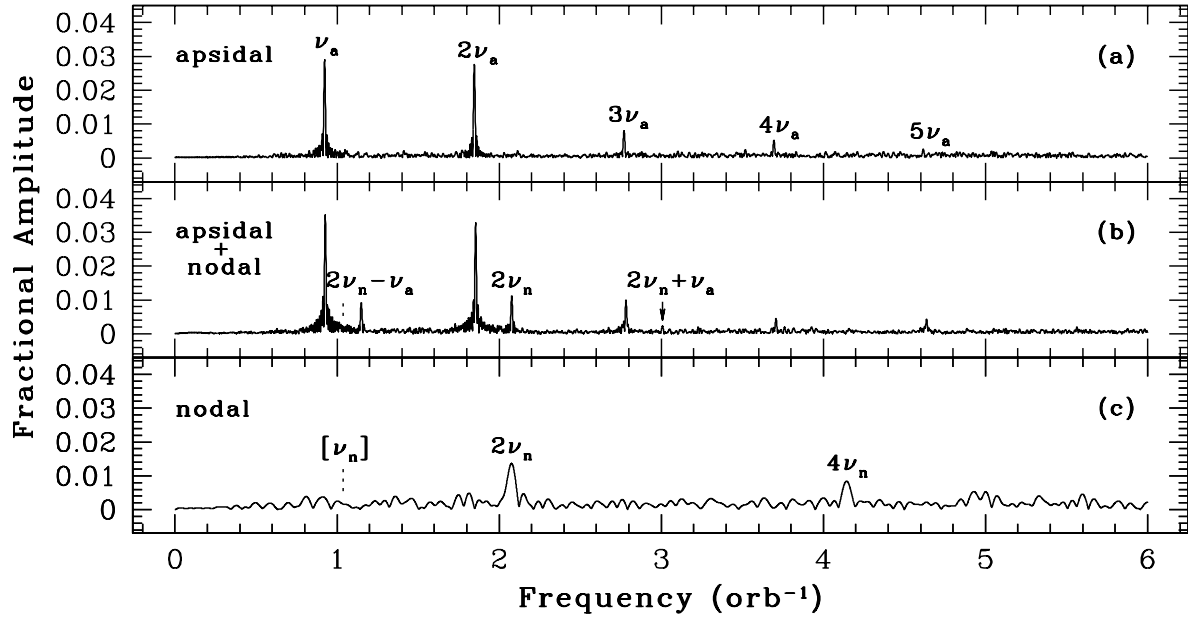


Fig. 2.— The top panel shows the Fourier amplitude spectrum of orbits 200 to 300 of the untilted reference disk. The middle panel shows the amplitude spectrum of orbits 200 to 300 of a disk tilted by 5° at orbit 200. In addition to the apsidal frequencies, there is now power at a peak labeled $2\nu_n$, and at the linear combination frequencies $2\nu_n - \nu_a$ and $2\nu_n + \nu_a$ (labels are centered over the peaks in all cases). The bottom panel shows the amplitude spectrum of orbits 50 to 70 of a disk tilted at orbit 40, well before apsidal superhumps develop. The driving frequency $2\nu_n$ and its harmonic are clearly evident. Observed nodal superhumps have frequencies ν_n one-half this frequency (dotted line), as we see only one side of an optically-thick disk in superoutburst.

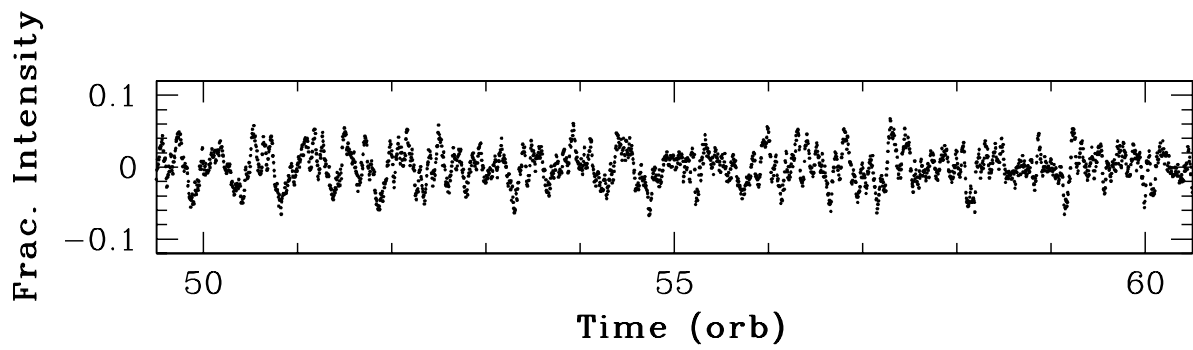


Fig. 3.— Boxcar-smoothed light curve showing nodal superhump oscillations (filter width is 11 points).

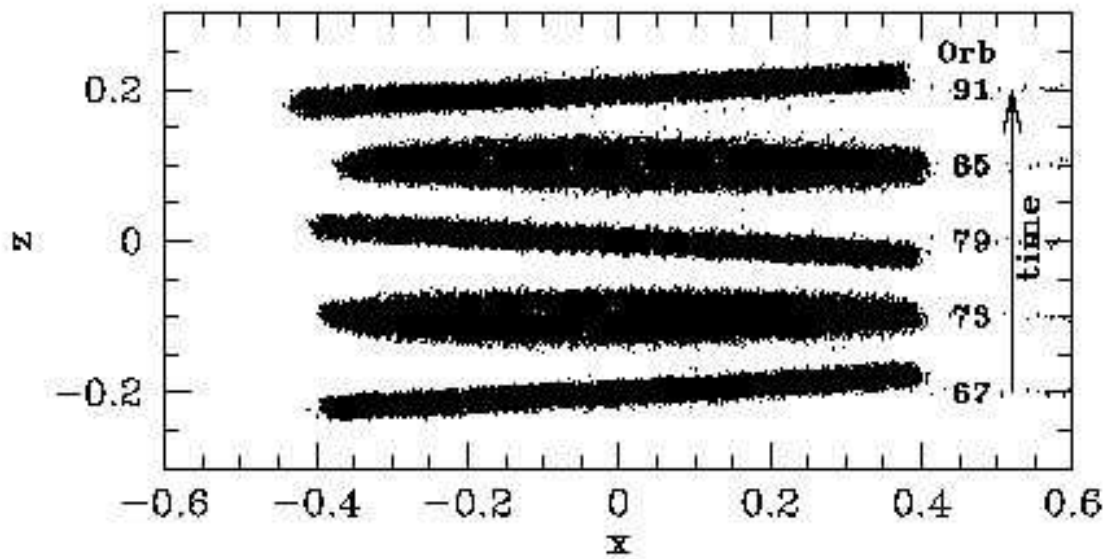


Fig. 4.— Sideview snapshots spanning one full nodal precession cycle of 24 orbits. The disk fluid has an angular momentum vector with a positive z component, but the tilted disk precesses in the opposite sense.